ISSN 8756-6990, Optoelectronics, Instrumentation and Data Processing, 2012, Vol. 48, No. 2, pp. 134–140. © Allerton Press, Inc., 2012.
Original Russian Text © S.G. Garanin, A.N. Manachinsky, F.A. Starikov, S.V. Khokhlov, 2012, published in Avtometriya, 2012, Vol. 48, No. 2, pp. 30–37.

OPTICAL INFORMATION TECHNOLOGIES

Phase Correction of Laser Radiation with the Use of Adaptive Optical Systems at the Russian Federal Nuclear Center—Institute of Experimental Physics

S. G. Garanin, A. N. Manachinsky, F. A. Starikov, and S. V. Khokhlov

Russian Federal Nuclear Center—Institute of Experimental Physics,
Institute of Laser Physics Research,
pr. Mira 37, Sarov, 607190 Russia
E-mail: fstar@mail.ru

Received October 28, 2011

Abstract—Results obtained at the Institute of Laser Physics Research (which is part of the Russian Federal Nuclear Center — Institute of Experimental Physics) on phase correction of pulsed and continuous wave laser radiation by closed-loop adaptive optical systems (AOS) with flexible deformable mirrors are described. With the help of a conventional AOS including a Hartmann–Shack wavefront sensor and an adaptive mirror having a 220×220 mm aperture, aberrations of the beam of a powerful pulsed laser facility called Luch have been reduced by an order of magnitude. The development of special software for reconstruction of singular wavefronts by the Hartmann–Shack sensor has allowed us to perform the correction of a doughnut-shaped Laguerre–Gaussian vortex laser beam in an AOS with a bimorph mirror and to focus it into a bright axial spot that drastically increases the Strehl ratio. Adaptive optical systems have been developed where the adaptive mirror control is ensured by searching for an extremum of a chosen criterion functional with the help of a stochastic parallel gradient algorithm rather than by means of wavefront measurements. Embedding of microcontrollers into the control unit has allowed us to reach an AOS bandwidth of 5 kHz and to demonstrate the dynamic phase correction of tip-tilts and higher aberrations of the wavefront caused by turbulence induced by heating of the beam propagation path under laboratory conditions.

Keywords: adaptive optical system, wavefront sensor, wavefront aberrations, phase correction.

DOI: 10.3103/S8756699012020045

INTRODUCTION

Application of adaptive optics for correction of laser radiation wavefront aberrations under static conditions allowed researchers to increase the beam quality in powerful pulsed lasers used to study laser radiation–matter interaction [1]. An increase in the efficiency of modern adaptive optical systems (AOS) appreciably expands the range of problem being solved in transporting powerful laser radiation in problems of location, communication, and optical processing of information. Two aspects of requirements to modern adaptive optical systems are particularly important [2]: first, it is necessary to ensure high accuracy of phase correction with due allowance for specific features of spatial distortions of the radiation wavefront (e.g., in a turbulent atmosphere); second, it is necessary to provide phase correction of the laser beam under dynamic conditions, i.e., the AOS has to operate fast enough to trace radiation phase changes and to correct them in due time.

AOS design requires three problems to be solved: determination of the general concept of AOS operation, choice of principles of controlling AOS elements, and provision of necessary optoelectronic facilities and elements (tip-tilt correctors, flexible adaptive mirrors, sensors for radiation parameters, feeding and control

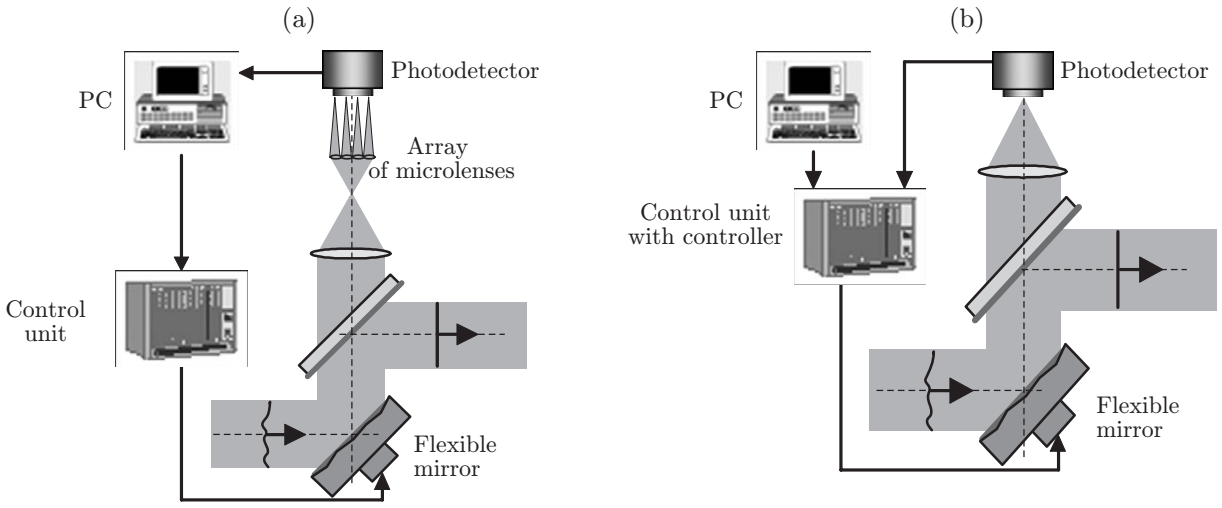

Fig. 1. AOS with a wavefront sensor (a) and sensorless AOS (b).

units, amplifiers, controllers, and special computers). These problems are interrelated and depend on the problem to be solved.

The experiments on adaptive phase correction of powerful laser beams having spatial specific features, which are described in this paper and which were performed at the Institute of Laser Physics Research (which is part of the Russian Federal Nuclear Center — Institute of Experimental Physics), were aimed at increasing the correction accuracy and speed with the use of two AOS types. In the first approach, we measured the phase surface of the beam by the Hartmann–Shack wavefront sensor (WFS); based on these measurements, the mirror surface was deformed accordingly. This system is commonly accepted and usually operates on the basis of the phase conjugation principle. In the second approach, phase front correction is based on different principles; it is performed on the basis of a blind approach with the use of an iterative stochastical parallel gradient algorithm of a predictor-corrector type, which includes searching for an extremum of a given criterion functional.

ADAPTIVE SYSTEMS WITH A WAVEFRONT SENSOR

The AOS with the Hartmann–Shack WFS is schematically shown in Fig. 1a. The WFS includes an array (ordered raster) of microlenses and a photodetector, which is a CCD camera whose screen is located in the focal plane of the microlens. The operation of the AOS with direct measurements of the phase surface by the WFS largely depends on the accuracy of wavefront measurements. The WFS includes diffractive multilevel arrays of microlenses fabricated by the kinoform technology (in-depth UV photolithography and chemical etching in a solution) [3]. The accuracy of microrelief fabrication determines the quality of the optical element and the accuracy of wavefront measurements. Each microlens ensures focusing characteristics with high stability of the parameters over the entire array area, which are close to diffraction-limited performance. The root-mean-square deviation of the step surface shape from a flat surface is within 5 nm (including the deepest level).

Figure 2 shows a typical Hartmann pattern and a phase surface of one laser beam reconstructed by the wavefront sensors with an 8-level array of microlenses and with a 16-level array containing 100×100 subapertures [4]. It is seen from the figure that halving the subaperture size allows us to reach higher resolution and to capture finer details of the phase front.

When the laser beam covers a sufficiently large distance in a turbulent atmosphere, the so-called regime of strong scintillations occurs [5]. In this regime, the optical field becomes speckled, and lines where the intensity vanishes and the neighboring wavefront regions acquire a helicoidal shape of screw dislocations are formed in the space along the beam axis. The vortex character of the beam can be easily detected in an experiment by analyzing the pattern of its interference with an obliquely incident plane wave: bands originate or vanish at the screw dislocation centers in the interferogram, i.e., the so-called “forks” are formed. The scintillation effects reduce the efficiency of energy transfer and distort information transferred by the light beam.

The conventional methods of wavefront measurements by the Hartmann–Shack WFS turned out to be actually unsuitable in the presence of vortices. A new technique was developed to reconstruct the singular

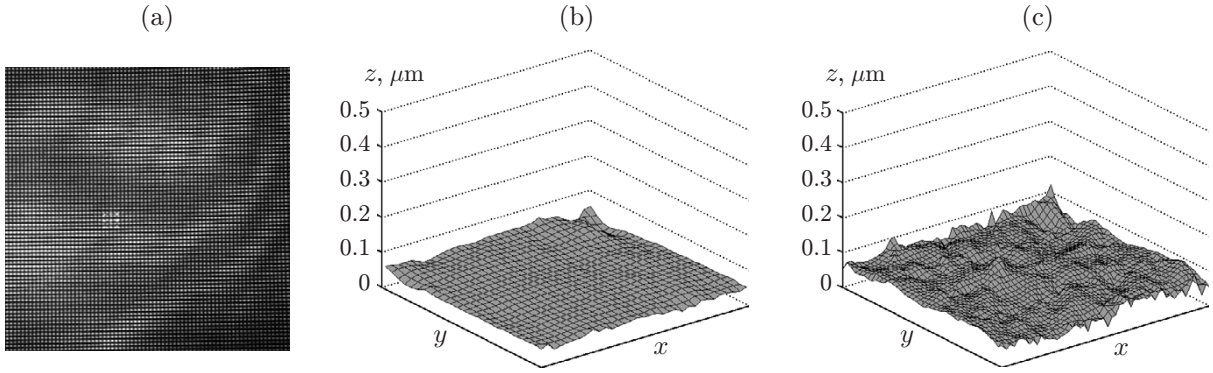

Fig. 2. Results of phase reconstruction: typical Hartmann pattern (a) and phase surface reconstructed at $\lambda = 0.65$ μm by the arrays of microlenses with a subaperture $d = 250$ μm and focal length $f = 20$ mm (b) and with a subaperture $d = 120$ μm and focal length $f = 5$ mm (c).

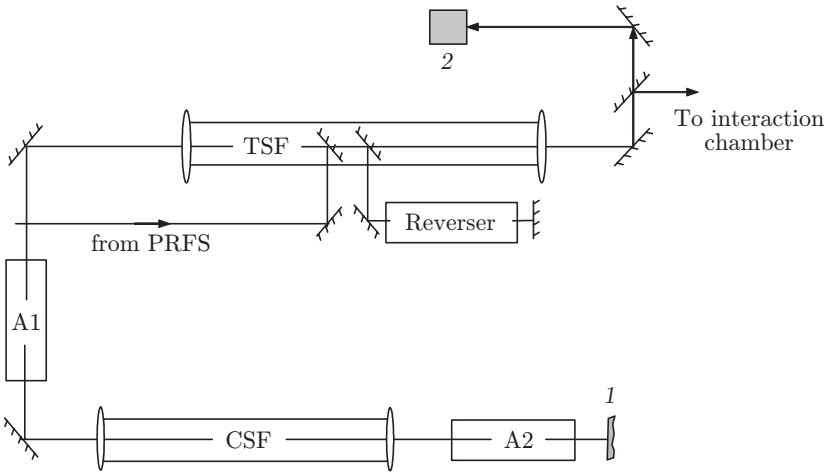

Fig. 3. Adaptive system in the Luch facility: adaptive mirror (*1*); output WFS (*2*); transport and cavity spatial filters (TSF and CSF); input pulse formation system (IPFS); amplifying stages (A1 and A2).

phase surface from the measured tilts of the phase front, and special software for the WFS was developed on the basis of this technique. Starikov et al. [6] recorded the wavefront of a specially formed optical vortex in the form of the Laguerre–Gaussian mode. The phase surface of the beam was reconstructed with the accuracy $\lambda/20$ ($\lambda = 0.65$ μm) for 8×8 spots in the Hartmann pattern.

Starikov et al. [7] demonstrated the correction of a vortex laser beam in a closed-loop AOS including the Hartmann–Shack sensor and a flexible bimorph mirror with the number of electrodes $(5\times5)+1$ [8]. It consists of two piezo-plates 0.4 mm thick, which are glued to an LK-105 glass substrate. One plate is continuous (i.e., it is one electrode); it is designed for compensation of defocusing. The second plate is divided into 5×5 8.5-mm electrodes with squared packing. The applied voltages range from -300 to $+300$ V. The experiments demonstrated that the bimorph adaptive mirror can correct the optical vortex in the practical sense, i.e., it can focus the doughnut-shaped vortex beam into a bright axial spot, which drastically increases the Strehl ratio and the resolution of the optical system.

An important parameter for powerful lasers used in studying problems of laser inertial confinement fusion is the radiation beam quality. Figure 3 shows the AOS as an element of the Luch 4-path laser facility on phosphate neodymium glass with a beam aperture of 200×200 mm and pulse duration of 3 ns, which was developed at the Institute of Laser Physics Research (which is part of the Russian Federal Nuclear Center — Institute of Experimental Physics) [9]. This facility includes a wide-aperture deformable adaptive mirror 220×220 mm with 61 piezo-electric actuators arranged in a squared geometry (turned at 45° with respect to the horizontal line) [10]. The applied voltages range from 0 to +120 V.

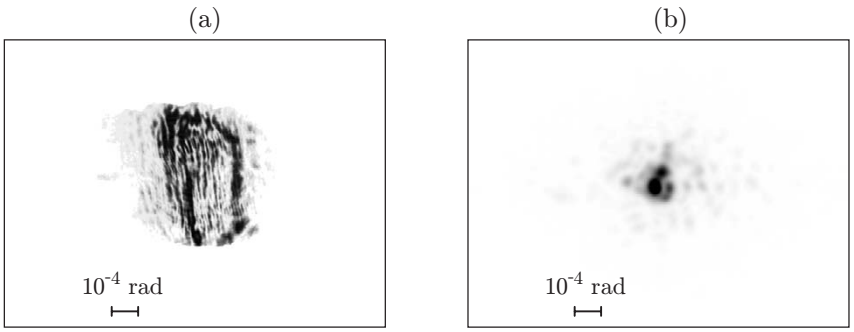

Fig. 4. Distribution of the energy density of output radiation in the far field before correction (a) and after correction (b).

The WFS working field was composed of 20×20 subapertures each $d = 200$ μm in size. An analysis of the output radiation phase front before the correction (with allowance for static and heat-induced active elements of dynamic aberrations) and after the correction shows that the magnitude of aberrations decreases from PV = 9.6 μm (PV is the maximum peak-to-valley deviation) and RMS = 2.4 μm (RMS is the root-mean-square deviation) to PV = 1.35 μm and RMS = 0.24 μm (i.e., by a factor of 7 in terms of PV and by a factor of 10 in terms of RMS). At RMS = 0.24 μm = 0.23λ and the ratio of the aperture size to the length of correlation of residual fluctuations of the phase equal to $3 \div 5$, the Strehl ratio is theoretically estimated as $0.2 \div 0.3$. An analysis of the energy density distributions in Fig. 4 shows that phase correction induces a four-fold decrease in divergence at the 80% level of energy: from $4 \cdot 10^{-4}$ to $1 \cdot 10^{-4}$ rad [11].

Note that similar values (PV = 1.5 μm and RMS = 0.18 μm) were obtained after the correction in the LMJ facility (France) [1] with an adaptive mirror having similar geometry of actuators, but a smaller number of them (39). The WFS had 64×64 subapertures. The output radiation energy density distribution in the far field was not given in [1].

SENSORLESS ADAPTIVE SYSTEMS

Wavefront reconstruction by the WFS is a complicated engineering problem. Moreover, because of locality of phase gradient measurements, their results are extremely sensitive to small-scale fluctuations of the phase. The problem is further aggravated by a weak signal, presence of a background, etc.

As was already noted, the AOS with the WFS yields the radiation wavefront, which is fairly similar to a plane front. As, under such conditions, the spot size in the far field should have the minimum possible value and the radiation brightness should be as high as possible, we can directly solve the problem of searching for an extremum of the corresponding criterion functional and skip wavefront measurements. An AOS with phase conjugation and without the WFS for continuous wave laser radiation is schematically shown in Fig. 1b.

The extremum search scheme should be iterative; therefore, the bandwidth of the system should be wide enough. The performance of the control unit in Fig. 1a is limited by the capabilities of the Windows operation system, which cannot work in the high-frequency regime. To increase the performance, we have to use a fast-response microcontroller. Therefore, the interface chip in the control unit was replaced by a microcontroller chip. For this reason, the personal computer in Fig. 1b is not involved into the feedback circuit: it is used only to start up the system and to change the microcontroller code prior to its operation if necessary. Specific features of the 32-bit microcontroller are the built-in high-speed flash memory and static memory, a large set of peripheral units and modules, and a large set of system functions decreasing the number of external components. For the microcontroller, there is a possibility of in-system re-programming of the built-in flash memory through a JTAG-ICE interface or a parallel interface on an external programmer unit. The built-in USB port allows applications that require a connection to a computer. The ARM command system can be processed well by compilers of high-level languages. The controller can operate at frequencies up to 55 MHz. This value is appreciably lower than the clock frequency of modern personal computers, but the commands are processed in the real-time regime, without delays of the Windows operation system, which significantly increases the control system operation speed. The controller also controls the power supply to the control unit. A single-element photodetector of radiation (photodiode or photoelectric multiplier) allows high-frequency performance, in contrast to the multielement CCD camera in Fig. 1a.

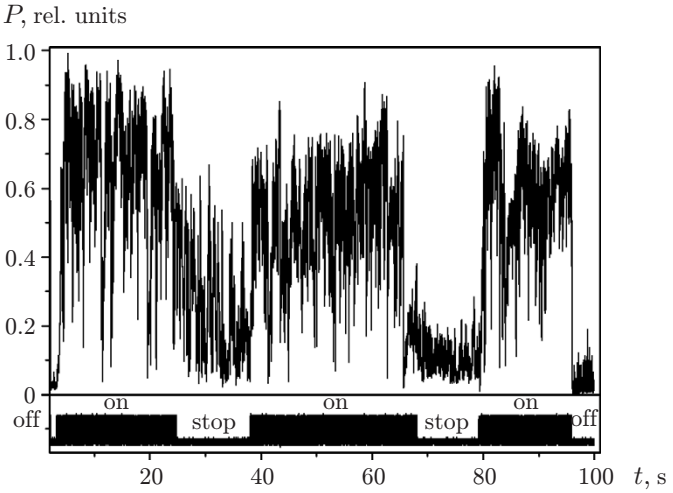

Fig. 5. Time evolution of the power of output radiation within a small angle.

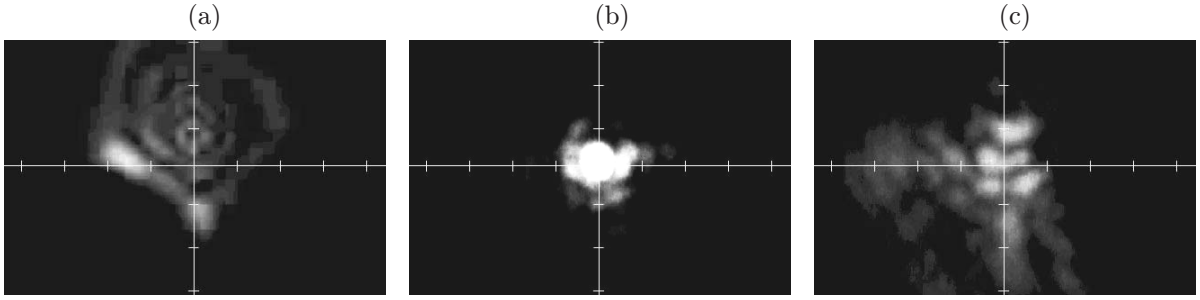

Fig. 6. Typical instantaneous distribution of output radiation in the far field for different states of the system: (a) off, (b) on, and (c) stop.

The proposed control algorithm, which involves a search for the extremum of the chosen criterion functional (in particular, the power of radiation within a given angle), is of the predictor–corrector type. The approach used here is similar to the algorithm of stochastic parallel gradient descent [12] in terms of the principle of parallel supply of voltage to the electrodes of the adaptive mirror and stochasticity of the first stage of the iteration. The algorithm is comparatively simple and, therefore, reliable and implementable. The operation of a sensorless adaptive system with the above-described bimorph adaptive mirror 45×45 mm [8] was demonstrated.

The frequency of the closed-loop operation cycle of the AOS equal to $3 \div 5$ kHz with optimal parameters of the algorithm was limited by the mechanical inertia of the adaptive mirror structure. The dynamic variation of the laser beam wavefront was ensured under laboratory conditions by a turbulent perturbation of the path with the use of a fan heater. The criterion functional was the power of radiation that passed through a diaphragm with a diffraction-order size, which was located ahead of the photodiode. The AOS could be in one of the three states: off (zero voltages on the electrodes), on (dynamically changing voltages in accordance with algorithmic commands issued by the controlled in the feedback regime), and stop (voltages reached at the stop instant are fixed during the stop period). Thus, we can observe the pattern of radiation in the far field distorted by aberrations during a desired time period in the off state, the dynamically corrected pattern of radiation in the on state, and the pattern of radiation with the correction of static aberrations (mainly) and without the correction of dynamic aberrations in the stop state.

Figure 5 shows the typical behavior of the power of output radiation within a given angle, i.e., the criterion functional, for a period of 100 s. The initial beam experiences dynamic distortions for which the signal power spectrum has a peak at the frequency of 7 Hz and considerable values in the frequency range up to 16 Hz. If the feedback is eliminated (off state), the signal level is rather weak. It is seen that the power increases by a factor of $20 \div 30$ when the feedback is restored (on state), then it decreases by a factor of $2 \div 4$ in the stop state, where only static aberrations are corrected. After that, the signal increases again

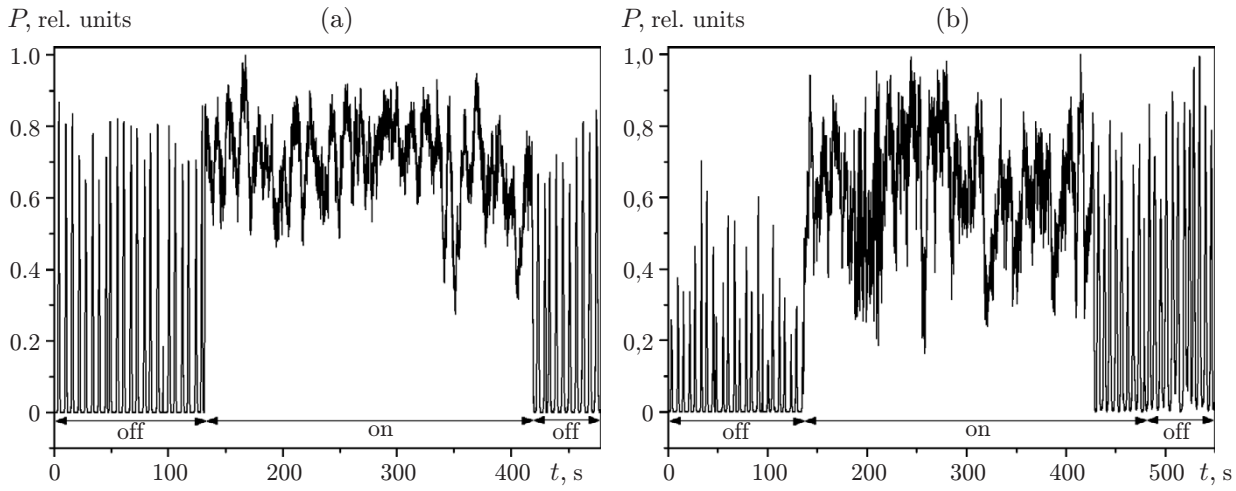

Fig. 7. Typical time evolution of the output radiation power within a given angle: the wavefront tilt frequency is 5 Hz (a) and 10 Hz (b).

when the feedback is restored (on state), etc., until feedback elimination (off state) finally leads to signal reduction to the initial low level. The instantaneous patterns of radiation in the far field for different AOS states are shown in Fig. 6.

The developed approach was also implemented in a situation where the flexible deformable mirror in the AOS was replaced by a tip-tilt corrector: a mirror 100 mm in diameter with two pushing piezo-actuators that ensured wavefront tilting in two directions (see Fig. 1b). A special control unit with an enhanced power was developed to control the corrector because of the large electric capacity of the pusher (6 μF), which allowed us to set the voltage on the pusher within several microseconds. The frequency of the closed-loop cycle of the system controlled by the controller was 1 kHz. It was determined by mechanical inertia of the corrector. A photoelectric multiplier with a diaphragm having a given angular size being mounted ahead of it was used as a photodetector. The system included a laser beam with periodic changes in the wavefront tilt in time, which corresponded to jitter of the focal spot in the diaphragm plane. A typical pattern of the output radiation power within a given angle for different frequencies of variations of the incoming beam wavefront tilt is shown in Fig. 7. When the feedback is switched on, the radiation beam in the diaphragm plane becomes stabilized and the mean level of the signal drastically increases.

CONCLUSIONS

In this paper, we demonstrated the results of using closed-loop AOS developed at the Institute of Laser Physics Research (which is part of the Russian Federal Nuclear Center — Institute of Experimental Physics) for phase correction of laser radiation, aimed at increasing the correction accuracy and operation speed. Adaptive mirror control based both on wavefront measurements by the Hartmann–Shack sensor and on the sensorless stochastic gradient algorithm with the search for the extremum of a chosen criterion functional is used. Using the first approach, we reduced aberrations of the beam of the powerful solid laser facility called Luch by an order of magnitude and obtained the residual root-mean-square error of correction equal to 0.24 μm. We also performed static correction of a singular vortex laser beam with accuracy of $\lambda/20$ and focused the beam into a bright axial spot, which drastically increased the Strehl ratio and the optical system resolution. Based on the second approach, the development of special control units with the use of microcontrollers allowed us to reach the AOS bandwidth of 5 kHz and to perform dynamic correction of wavefront aberrations induced by turbulent owing to path heating under laboratory conditions by using a flexible bimorph mirror with a 45-mm aperture having 25 control element.

REFERENCES

1. C. Grosset-Grange, J.-N. Barnier, C. Chappuis, and H. Cortey, "Design Principle and First Results Obtained on the LMJ Deformable Mirror Prototype," Proc. SPIE **6584**, 658403 (2007).

2. V. P. Lukin, "Selection of Basic Parameters of Adaptive Optical Systems," Avtometriya **48** (2), 3–11 (2012) [Optoelectron., Instrum. Data Process. **48** (2), 111–118 (2012)].
3. V. V. Atuchin, V. V. Soldatenkov, A. V. Kirpichnikov, et al., "Multilevel Kinoform Microlens Arrays in Fused Silica for High-Power Laser Optics," Proc. SPIE **5481**, 43–46 (2004).
4. F. A. Starikov, V. V. Atuchin, M. O. Koltygin, et al., "Multilevel Lenslet Arrays in Precise Hartmann-Shack Wavefront Sensing of Laser Beam," in *EOS Annual Meeting, 2010*, Paper TOM4-3188-22, pp. 80.
5. D. L. Fried and J. L. Vaughn, "Branch Cuts in the Phase Function," Appl. Opt. **31** (15), 2865–2882 (1992).
6. F. A. Starikov, G. G. Kochemasov, S. M. Kulikov, et al., "Wave Front Reconstruction of an Optical Vortex by Hartmann-Shack Sensor," Opt. Lett. **32** (16), 2291–2293 (2007).
7. F. A. Starikov, G. G. Kochemasov, M. O. Koltygin, et al., "Correction of Vortex Laser Beam in a Closed-Loop Adaptive System with Bimorph Mirror," Opt. Lett. **34** (15), 2264–2266 (2009).
8. F. A. Starikov, V. P. Aksenov, V. V. Atuchin, et al., "Wave Front Sensing of an Optical Vortex and its Correction in the Close-Loop Adaptive System with Bimorph Mirror," Proc. SPIE **6747**, 6747OP (2007).
9. I. N. Voronich, I. V. Galakhov, S. G. Garanin, et al., "Measurements of the Amplification Coefficient in a Disk Amplifying Stage with Active Elements Made of Neodymium Phosphate Glass," Kvant. Elektron. **33** (6), 485–488 (2003).
10. S. G. Garanin, S. V. Grigorovich, S. M. Kulikov, et al., "Deformable Mirror Based on Piezo-Electric Drives for the Adaptive System of the Iskra-6 Facility," Kvant. Elektron. **37** (8), 691–696 (2007).
11. S. G. Garanin, S. M. Kulikov, A. N. Manachinsky, et al., "Development of an Adaptive System. Experimental Results Obtained in the Luch Facility," in *Abstracts of XXXVII Intern. Conf. on Plasma Physics and Controlled Thermonuclear Fusion* (Plazmaiofan, Moscow, 2010), p. 142.
12. M. Vorontsov, J. Riker, G. Carhart, et al., "Deep Turbulence Effects Compensation Experiments with a Cascaded Adaptive Optics System Using a 3.63 m Telescope," Appl. Opt. **48** (1), A47–A57 (2009).